Chinese Chemical Letters 31 (2020) 1807–1811

Contents lists available at ScienceDirect

Chinese Chemical Letters

journal homepage: www.elsevier.com/locate/cclet

Communication

Anti-inflammatory catecholic chitosan hydrogel for rapid surgical trauma healing and subsequent prevention of tumor recurrence

Gang He[a,1], Xu Yan[b,1], Zhaohua Miao[a,1], Haisheng Qian[c], Yan Ma[a,*], Yan Xu[a], Li Gao[a], Yang Lu[b,*], Zhengbao Zha[a,*]

[a] School of Food and Biological Engineering, Hefei University of Technology, Hefei 230009, China
[b] School of Chemistry and Chemical Engineering, Hefei University of Technology, Hefei 230009, China
[c] School of Biomedical Engineering, Research and Engineering Center of Biomedical Materials, Anhui Medical University, Hefei 230032, China

ARTICLE INFO

Article history:
Received 11 December 2019
Received in revised form 14 February 2020
Accepted 17 February 2020
Available online 18 February 2020

Keywords:
Surgery
Anti-inflammation
Bactericidal capacity
Trauma healing
Tumor recurrence

ABSTRACT

Although occupying pillar position in clinical cancer treatments, surgery itself and surgical trauma would elicit series of local/systemic inflammation-related responses that resulted in high rate of tumor recurrence. Herein, chitosan with conjugated gallic acid (CSG) molecules were coordinated with Fe^{3+} to form CSG/Fe^{3+} hydrogel for filling the tumor-resected cavity with considerable wet-adhesion ability and anti-inflammatory performance. With the assistance of doxorubicin hydrochloride (DOX·HCl), CSG/Fe^{3+}/DOX hydrogel exhibited synergistic photothermal-chemo tumor-inhibited performance under near-infrared (NIR) light irradiation for eradicating residual and/or surgical trauma-recruited cancer cells. Thus, our study attempts to show a paradigm that realizes quick surgical trauma healing, inflammation inhibition and prevention of postsurgical tumor recurrence.

Despite various emerging therapeutics have been developed in animal models [1–6], surgery remains a mainstay in clinic (> 60% of patients are treated with surgery) for removing primary or metastatic tumors [7–10]. Nevertheless, surgical excision still encounters the dilemma that patients who undergo cancer resection do not survive as long as expected [11–14]. In addition to the incomplete tumor removal, cascades of local/systemic inflammation triggered by surgical traumas would capture cancer cells and support their survival and even metastatic growth [15,16]. Therefore, quickly healing the irregular injury with diminished inflammation are essential to decrease the surgery-induced acceleration of tumor growth. Although the administration of chemotherapeutics in perioperative period has been reported to be beneficial for prolonging long-term survival currently, the cancer patients always suffer from serious side effects [17–21]. Thus, developing tissue adhesives with anti-inflammation capacities for locoregional drug delivery in surgical traumas are thus highly pursued.

Recently, suffering from reduced electrostatic attraction forces as well as van der Waals force [22], hydrogel-based tissue adhesives commonly compromised low tissue adhesion. Delightingly, marine mussels are known to exhibit rapid, tough and long-lasting adhesion to various substrates under wet conditions owing to the two main components of catecholic amino acid (3,4-dihy-droxyphenylalanine, DOPA, abbreviated Y) and L-lysine (abbreviated K) in their byssus secretions (primary amino acid sequence of mussel foot proteins (*Mfp*)*-3* and *Mfp-5* are ADYYGPNYGPPRRYGGGNYNRYNRYGRRYG-GYKGWNNGWNRGRRGKYW and SSEEYKGGYYPGNAYHYHSGGSY HGSGYHGGYKGKYYGKAKKYYYKYKNSGKYKLKKARKYHRKGYKYYG GSS, respectively) [23,24]. Bioinspired from this adhesion mechanism, mussel-inspired hydrogel with robust adhesion ability would provide an effective approach to overcome the limitation of wet-suppression adhesion [25]. Yet, one self-contradictory situation is that hydrogels with firm adhesive capacity would also easily adsorb pathogenic bacteria, which could trigger wound infection, inflammation and further immune responses [26,27]. So far, it is still a major challenge of surgical tissue adhesives to possess considerable wet tissue-affinity and considerable anti-infection performance simultaneously.

Motivated by well-reported catechol-Fe^{3+} chemistry [28,29], a mussel-inspired catecholic chitosan hydrogel was developed here as a multifunctional surgical tissue adhesive with excellent anti-inflammatory and tumor inhibition capacities. Chitosan (CS) with

* Corresponding authors.
E-mail addresses: yanma@hfut.edu.cn (Y. Ma), yanglu@hfut.edu.cn (Y. Lu), zbzha@hfut.edu.cn (Z. Zha).
[1] These authors contributed equally to this work.

https://doi.org/10.1016/j.cclet.2020.02.032
1001-8417/

conjugated gallic acid (GA) molecules (CSG) were chelated with Fe^{3+} and doxorubicin hydrochloride (DOX·HCl) to generate CSG/Fe^{3+}/DOX hydrogel, which was hypothesized to have considerable adhesive affinity to moist surgical traumas. Furthermore, the obtained CSG/Fe^{3+}/DOX hydrogel would display acidic pH and near-infrared (NIR) light promoted DOX release profiles, following a synergistic cancer cell killing effect for preventing tumor recurrence.

Under the assistance of hydroxybenzotriazole (HOBt), CS was dissolved in DI water at ambient environment. After the addition of GA and 1-ethyl-3-(3′-dimethylaminopropyl) carbodiimide hydrochloride (EDC·HCl) for 24 h, the CSG powder could be obtained after a typical dialysis and freeze-drying process (Fig. 1a). According to the reported method [30], the degree of catechol conjugation in CSG was calculated to be 21.5% (with a feeding molar ratio of GA to CS repetitive unit to be 1:4) by comparing the relative peak area of a catechol group (3H, aromatic ring proton, δ 6.87, D_2O) and an acetyl group (3H, —$COCH_3$, δ 1.92, D_2O) on a CS backbone (Fig. S1 and Table S1 in Supporting information). As shown in Fig. 1b, no significant cytotoxicity was observed after treating HUVECs with CSG up to 500 μg/mL for 24 h. Interestingly, low concentrated CSG solutions (< 100 μg/mL) exhibited a growth-promoting effect to HUVECs, similar to the well-reported endothelial cell growth promoting effect of CS [31–33]. Unlike friendly to HUVECs, the selective tumor cell-inhibition activity of GA by their reducing phenolic hydroxyl groups also endowed CSG with the slight cancer cell (4T1 breast cancer cells were used here) killing ability [34,35], which is beneficial for erasing the tumor cells and promoting wound healing in surgical trauma. Furthermore, H_2O_2 and lipopolysaccharides (LPS) were both used to establish intracellular reactive oxygen species (ROS) threats in HUVECs to mimic postsurgical inflammation. Not surprisingly, H_2O_2 or LPS would result in elevated mortality of HUVECs while cell viability could be significantly increased with co-incubation of CSG (100 μg/mL), indicating the cell-protective effect of CSG (Figs. 1c and d).

Another mortal threat during postoperation period is bacterial infection, thus conventional Gram-negative *Escherichia coli* (*E. coli*) and Gram-positive methicillin-resistant *Staphylococcus aureus* (*MRSA*) were both employed as model bacteria to test the antibacterial efficacy of CSG molecule before its further *in vivo* implantation. After incubated with CSG aqueous solution for 24 h, viable bacteria counts were estimated by the spread plate method and the plates were incubated at 37 °C for 24 h followed with colonies counting. As shown in Figs. 1e and f, catechol-conjugated CSG exhibited a dose-dependent bacterial-inhibiting ability. In detail, the minimum concentration of CSG for completely inhibiting *E. coli* and *MRSA* was around 250 and 500 μg/mL, respectively. Therefore, CSG molecule still retain considerable antibacterial ability from CS and GA which was necessary for *in vivo* anti-infection applications.

Due to the catechol-Fe^{3+} interfacial bond dynamics, mixing aqueous CSG and Fe^{3+} solutions with an optimal molar ratio would result in CSG/Fe^{3+} hydrogel (Fig. 2a). Considering the demand of shape-maintaining ability and injectability for surgical trauma filling, CSG/Fe^{3+} hydrogel formed by mixing CSG (30 mg/mL) and Fe^{3+} (25 mmol/L) solution was preferentially selected for further use (Fig. 2b). The framework of CSG/Fe^{3+} hydrogel exhibited a homogeneous porous structure and element distribution of C and Fe, indicating an uniform catechol-Fe^{3+} crosslinkage (Fig. S2 in Supporting information) and high water content (around 0.93 ± 0.2 g of water per 1.0 mL of CSG/Fe^{3+} hydrogel, Fig. S3 in Supporting information). In addition, the existence of Fe in CSG/Fe^{3+} hydrogel was confirmed by two broad binding energy peaks around 711 and 724 eV which were ascribed to the Fe $2p_{3/2}$

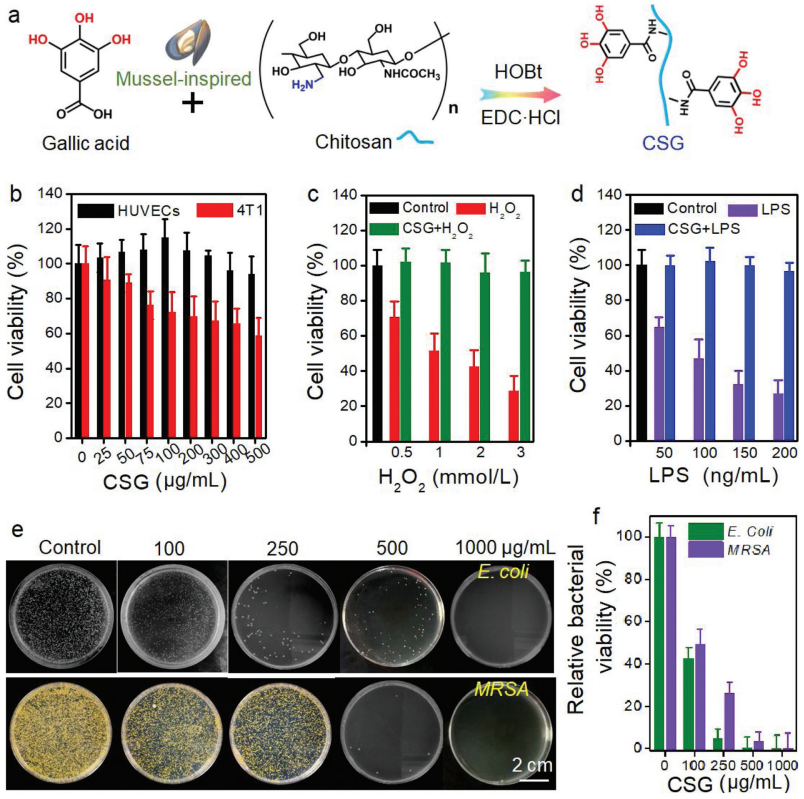

Fig. 1. Characterization of CSG molecule. (a) Synthetic route for CSG molecules; (b) cytotoxicity of CSG on HUVECs and 4T1 cancer cells, respectively; quantitative detection of HUVECs viability when treated with H_2O_2 (c) and LPS (d); antibacterial activity of CSG against *E. Coli* and *MRSA*: (e) digital photographs and (f) the corresponding calculated relative antibacterial ratio.

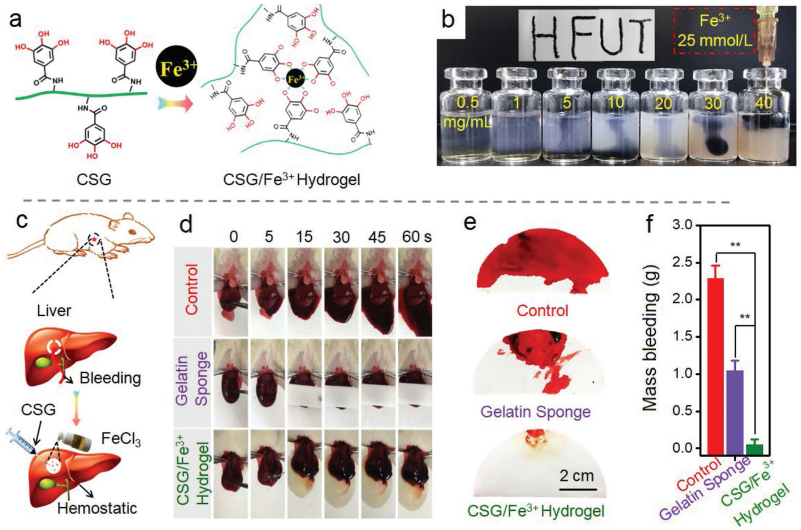

Fig. 2. Characterization of CSG/Fe^{3+} hydrogel: (a) well-reported catechol-Fe^{3+} interfacial bond dynamics; (b) photographs of CSG/Fe^{3+} hydrogel and depiction of HFUT (abbreviation for Hefei University of Technology); (c) schematic depiction of building rat liver bleeding model; (d) partial view of the bleeding rat liver at predetermined time; (e) typical bloody filter papers and (f) weight of blood loss for various treated groups. ** $P < 0.01$.

and Fe $2p_{1/2}$ with various valences, indicating the co-existence of Fe^{2+} and Fe^{3+} in CSG/Fe^{3+} hydrogel due to the redox-reaction between catachol and Fe^{3+} (Fig. S4 in Supporting information). Before *in vivo* surgical trauma filling, the cytotoxicity of CSG/Fe^{3+} hydrogel was evaluated by hemocompatibility and cytocompatibility studies. As shown in Figs. S5 and S6 in Supporting information, nearly non-toxic effect could be oberservd for CSG/Fe^{3+} hydrogel.

After building a rat liver bleeding model (Fig. 2c), CSG/Fe^{3+} hydrogel (*in situ* formed by subsequent injection of CSG and Fe^{3+} solutions) and clinically-used gelatin sponge were both employed for comparing their hemostatic abilities. As shown in Fig. 2d, the time to achieve efficient hemostasis of CSG/Fe^{3+} hydrogel (around 5 s) is much shorter than gelatin sponge (around 30 s), indicating the better hemostatic performance of as-prepared CSG/Fe^{3+} hydrogel. After bleeding from the liver cut for 60 s (the time for stopping bleeding without any treatment: control group), the CSG/Fe^{3+} hydrogel treated group showed significantly reduced blood loss from either the perspective of bleeding area (Fig. 2e) or weight (Fig. 2f).

Due to the high catechol and water content in CSG/Fe^{3+} hydrogel, we deduced that hydrophilic DOX·HCl could be efficiently encapsulated in CSG/Fe^{3+} hydrogel to form CSG/Fe^{3+}/DOX hydrogel through π-π interactions and the obtained DOX loaded hydrogel was supposed to show both pH-dependent and NIR light irradiation promoted DOX release fashions (Fig. 3a). The increased repulsive

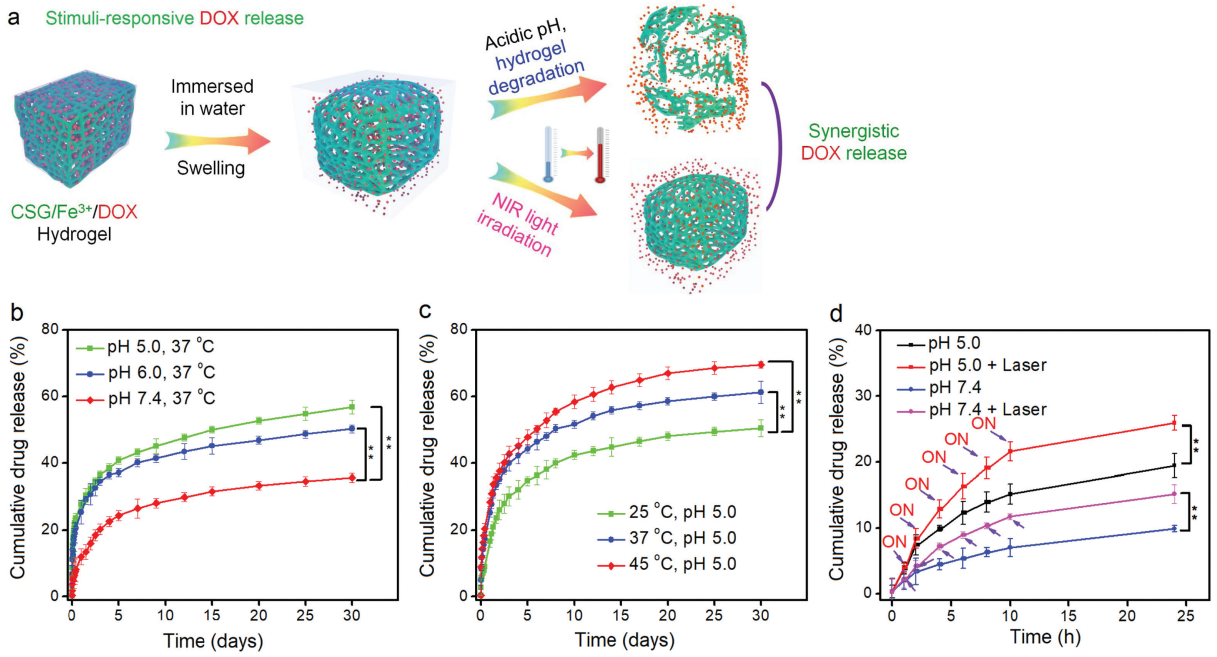

Fig. 3. Stimuli-responsive DOX release properties. (a) Schematic depiction of potential pH/NIR light dependent DOX release profiles; (b) DOX release behaviors in PBS with different pH; (c) temperature influence on DOX release in PBS with pH 5.0; (d) NIR light irradiation promoted DOX release. ** $P < 0.01$.

force between protonated amino residues in CSG backbone and DOX molecules as well as higher solubility guaranteed the acidic pH promoted DOX release profiles (nearly 35.6%, 50.2% and 56.7% of loaded DOX could be released in PBS with pH of 7.4, 6.0 and 5.0 for 30 days, respectively) of CSG/Fe^{3+}/DOX hydrogels (Fig. 3b). Thus, on account of the increased lactic acid generation of tumor, CSG/Fe^{3+}/DOX hydrogels could serve as a tumor-prefered long-lasting drug release system. Moreover, as shown in Fig. 3c and Fig. S7 (Supporting information), CSG/Fe^{3+}/DOX hydrogels also showed heat-accelerating DOX release properties in PBS with both pH values of 7.4 and 5.0.

Next, well-reported photothermal conversion performance of catechol-Fe^{3+} related products also motivated us to confirm the thermosensitivity of CSG/Fe^{3+}/DOX hydrogels [36]. Under the irradiation of near infrared (NIR) light, the hydrogel exhibited good photothermal-induced temperature elevation in both time-dependent and power densities-dependent manners (Fig. S8 in Supporting information). After five discontinuous NIR light irradiations (808 nm, 1.5 W/cm^2, 10 min), at least 6% increment of released DOX could be realized in only 24 h release period in PBS with pH values of either 7.4 or 5.0 (Fig. 3d). Thus, the above results demonstrated that CSG/Fe^{3+}/DOX hydrogel could be utilized as a both acidic pH and NIR light responsive DOX release system.

In light of the above acidic-pH and NIR light promoted drug release performance, the *in vivo* prevention capacity of local tumor recurrence of CSG/Fe^{3+}/DOX hydrogel was further investigated. A 4T1 breast tumor local recurrence model was further established by excising all the visible tumor tissues with average volume of 60 mm^3 and the resulted surgical trauma was then filled with 100 μL of as-prepared hydrogel or PBS (Fig. 4a). Under 10 min mild NIR light irradiation (0.5 W/cm^2, 808 nm), the temperature of surgical trauma could reach ~46 °C for all the hydrogel + NIR groups while only ~32 °C for PBS + NIR group (Fig. 4b and Fig. S9 in Supporting information), further verifying the good *in vivo* photothermal conversion effect of catechol-Fe^{3+} based hydrogels. After various treatments, the tumor volume and body weight of treated mice as well as stained tumor slices were monitored to verify the therapeutic outcomes. Notably, surgical excision commonly could not realize complete tumor inhibition due to the residue or recruitment of cancer cells. As shown in Fig. 4c and Fig. S10 (Supporting information), postoperative mice treated with PBS + NIR experienced fast tumor recurrence with 16 days while CSG/Fe^{3+} hydrogel filling could slightly delay the recurrence rate, confirming the mild tumor inhibiting ability of catechol conjugated CSG molecules. The CSG/Fe^{3+}/DOX hydrogel and CSG/Fe^{3+} hydrogel + NIR treated groups both exhibited better prevention of 4T1 cancer recurrence with decreased recurrent tumor volume for more than two weeks. As expected, the postsurgical mice treated with CSG/Fe^{3+}/DOX hydrogel + NIR group did not show any detectable tumor recurrence. In addition, detectable nuclei broken or shrinking was found in tumor slices treated with CSG/Fe^{3+}/DOX hydrogel, CSG/Fe^{3+} hydrogel + NIR and CSG/Fe^{3+}/DOX hydrogel + NIR (Fig. 4d), while no significant body weight loss and pathological change in fatal organs (Figs. S11 and S12 in

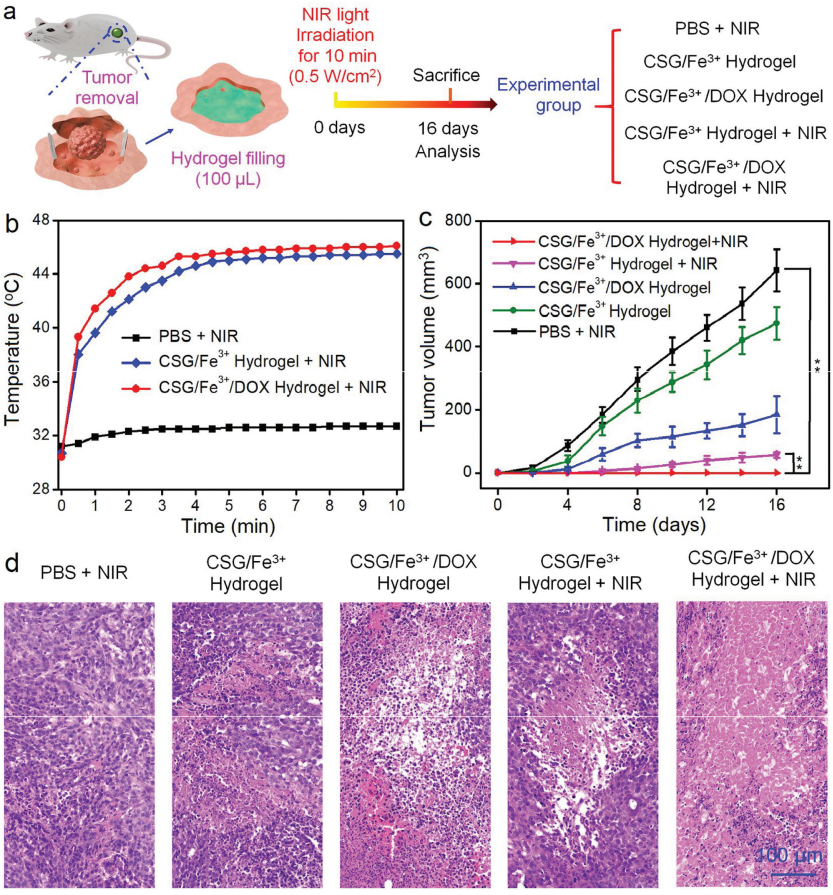

Fig. 4. Effective prevention of tumor recurrence of CSG/Fe^{3+}/DOX hydrogel: (a) schematic illustration of establishing 4T1 breast tumor local recurrence model and grouping of *in vivo* surgical trauma treatment; (b) temperature changes of mice under NIR laser irradiation; (c) volume of recurrent tumor and (d) H&E staining images of tumor slices immediately after various treatments. ** $P < 0.01$.

Supporting information) and was occurred during the whole treatment period, further indicating no unacceptable toxicity of as-prepared hydrogels. Thus, the obtained results together support the hypothesis that CSG/Fe^{3+}/DOX hydrogel could prevent post-surgical tumor recurrence efficiently *in vivo* through synergistic photothermal-chemo therapy.

In conclusion, mussel-mimic CSG/Fe^{3+} hydrogel has been successfully developed to avoid postsurgical tumor recurrence with excellent hemostatic performance, anti-inflammatory and antibacterial behaviors. After encapsulating chemotherapeutical DOX·HCl, the obtained CSG/Fe^{3+}/DOX hydrogel possessed acidic pH and NIR light irradiation promoted DOX release profiles which were beneficial to realize synergistic photothermal-chemo prevention of surgey-related tumor recurrence.

Declaration of competing interest

The authors declare that they have no known competing financial interests or personal relationships that could have appeared to influence the work reported in this paper.

Acknowledgments

This work was financially supported by the National Natural Science Foundation of China (Nos. 31800834, 51572067), the University Synergy Innovation Program of Anhui Province (No. GXXT-2019-045) and the Fundamental Research Funds for the Central Universities (Nos. JZ2018HGPA0273, JZ2018HGPA0269, JZ2018HGTB0247).

Appendix A. Supplementary data

Supplementary material related to this article can be found, in the online version, at doi:https://doi.org/10.1016/j.cclet.2020.02.032.

References

[1] V.P. Chauhan, R.K. Jain, Nat. Mater. 12 (2013) 958–962.
[2] D. Rosenblum, N. Joshi, W. Tao, J.M. Karp, D. Peer, Nat. Commun. 9 (2018) 1410.
[3] Z.H. Miao, S. Chen, C.Y. Xu, et al., Chem. Sci. 10 (2019) 5435–5443.
[4] G. He, S. Chen, Y.J. Xu, et al., Mater. Horiz. 6 (2019) 711–716.
[5] D. Wu, X. Duan, Q. Guan, et al., Adv. Funct. Mater. 29 (2019) 1900095.
[6] K. Ding, C. Zheng, L. Sun, et al., Chin. Chem. Lett. 31 (2020) 1168–1172.
[7] S. Tohme, R.L. Simmons, A. Tsung, Cancer Res. 77 (2017) 1548–1552.
[8] Q. Chen, C. Wang, X. Zhang, et al., Nat. Nanotechnol. 14 (2019) 89–97.
[9] H.J. Chen, Y. Ma, X.W. Wang, Z.B. Zha, J. Mater. Chem. B 5 (2017) 7051–7058.
[10] J.G. Hiller, N.J. Perry, G. Poulogiannis, B. Riedel, E.K. Sloan, Nat. Rev. Clin. Oncol. 15 (2018) 205–218.
[11] M. Horowitz, E. Neeman, E. Sharon, S.B. Eliyahu, Nat. Rev. Clin. Oncol. 12 (2015) 213–226.
[12] R. Demicheli, M. Retsky, W. Hrushesky, M. Baum, I. Gukas, Ann. Oncol. 19 (2008) 1821–1828.
[13] J. Coffey, M. Smith, J. Wang, et al., Bioessays 28 (2006) 433–437.
[14] J. Shao, C. Ruan, H. Xie, et al., Adv. Sci. 5 (2018) 1700848.
[15] S.M. Murthy, R.A. Goldschmidt, L.N. Rao, et al., Cancer 64 (1989) 2035–2044.
[16] S. Tohme, H.O. Yazdani, A.B. Al-Khafaji, et al., Cancer Res. 76 (2016) 1367–1380.
[17] J. van der Hage, C. van de Velde, J.P. Julien, et al., Eur. J. Cancer 37 (2001) 2184–2193.
[18] H.J. Chen, Y. Ma, X.W. Wang, X.Y. Wu, Z.B. Zha, RSC Adv. 7 (2017) 248–255.
[19] Q. Li, J. Wen, C. Liu, et al., ACS Biomater. Sci. Eng. 5 (2019) 768–779.
[20] Y. Qi, H. Min, A. Mujeeb, et al., ACS Appl. Mater. Interfaces 10 (2018) 6972–6981.
[21] S.L. Leung, Z.B. Zha, W.B. Teng, et al., Soft Matter 8 (2012) 5756–5764.
[22] M. Krogsgaard, V. Nue, H. Birkedal, Chem. -Eur. J. 22 (2016) 844–857.
[23] M. Liao, P. Wan, J. Wen, et al., Adv. Funct. Mater. 27 (2017) 1703852.
[24] R. Wang, J. Li, W. Chen, et al., Adv. Funct. Mater. 27 (2017) 1604894.
[25] L. Han, K. Liu, M. Wang, et al., Adv. Funct. Mater. 28 (2018) 1704195.
[26] X. Zhao, H. Wu, B. Guo, et al., Biomaterials 122 (2017) 34–47.
[27] Y. Huang, H. Li, X. He, et al., Chin. Chem. Lett. 31 (2020) 787–791.
[28] Q. Li, D.G. Barrett, P.B. Messersmith, N.H. Andersen, ACS Nano 10 (2016) 1317–1324.
[29] H. Ejima, J.J. Richardson, K. Liang, et al., Science 341 (2013) 154–157.
[30] J.H. Ryu, Y. Lee, W.H. Kong, et al., Biomacromolecules 12 (2011) 2653–2659.
[31] L.L. Chiu, M. Radisic, J. Control. Release 155 (2011) 376–385.
[32] F. Du, H. Wang, W. Zhao, et al., Biomaterials 33 (2012) 762–770.
[33] R. Huang, W. Li, X. Lv, et al., Biomaterials 53 (2015) 58–75.
[34] P. Darvin, Y.H. Joung, D.Y. Kang, et al., J. Cell. Mol. Med. 21 (2017) 720–734.
[35] L.H. Russell, E. Mazzio, R.B. Badisa, et al., Anticancer Res. 31 (2011) 3739–3745.
[36] L. An, C. Yan, X. Mu, et al., ACS Appl. Mater. Interfaces 10 (2018) 28483–28493.